Results of Subscale MTF Compression Experiments

Stephen Howard, Alex Mossman, Mike Donaldson and the General Fusion Team

General Fusion Inc., Burnaby, British Columbia, Canada

APS DPP Conference San Jose, California Oct. 31- Nov. 5, 2016 **CP10.00104**

INTRODUCTION

Concept

- In magnetized target fusion (MTF) a magnetized plasma torus is compressed in a time shorter than its own energy confinement time (adiabatic), thereby heating to fusion conditions.
- Understanding plasma behavior and scaling laws under these conditions is needed to advance toward a reactor-scale demonstration.
- General Fusion[1] is conducting a sequence of compression experiments on subscale compact toroid (CT) plasmas using a chemically driven aluminum liner. We call these *PCS* tests (for *Plasma Compression Small*)
- PCS experiments are tests of our MTF compression scheme. Compression in future power plant designs will use a collapsing liquid metal vortex.
- CT plasmas are formed by a coaxial Marshall gun, with magnetic fields supported by internal plasma currents and eddy currents in the wall.
- *PCS* experimental systems are built in a set of mobile containers to enable transport to the site where compression experiments are done.
- Two mobile systems exist and alternate between in-lab development and field deployment, they are called: Magnetized Ring Test (MRT) and Magnetized Ring Sustainment Test (MRST)
- Configurations that have been compressed so far include decaying and sustained spheromaks and spherical tokamak (ST) plasmas that are formed into a pre-existing toroidal field.
- Before compression the CT has an energy of ~10kJ magnetic, ~1 kJ thermal, with T_e ~ 100 – 400 eV, n_e ~ 1-5x10^{20} m^{-3}.
- A reactor scale demonstration would require ~10x higher initial B and n_e but similar T_e.
- Lawson criteria for MTF depends on the inertial dwell time at peak density and temperature.

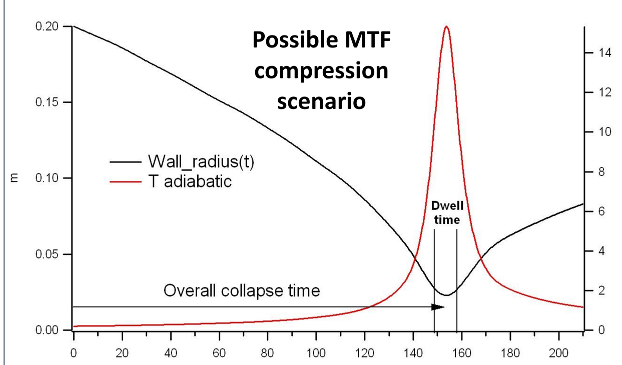

- Compression design improvements has eliminated tearing and minimized ripple and ejection of micro-debris
- Diagnostics measure B, n_e, visible, x-ray and neutron emission, T_i and T_e (TS in lab-only).
- Plasma was stable during a compression factor R_0/R >3 on best shots.
- Compression R_0/R ~ 10 is typical of most MTF scenarios.

Theoretical scaling laws for MTF compression

It is typically useful to describe an MTF system in terms of a radial compression factor, where *R(t)* is a characteristic radius of the system and R_0 is the initial value.

$$C_R = \frac{R_0}{R(t)}$$

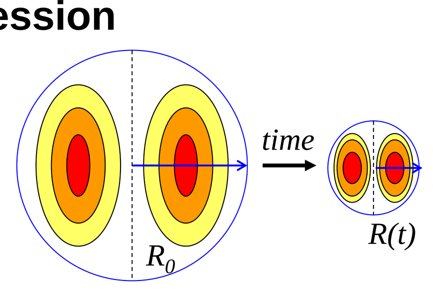

- **Ideal spherical scaling, uniform profile**, $\gamma = 5/3$

$$\frac{n(t)}{n_0} = C_R^3 \quad \frac{T(t)}{T_0} = C_R^2 \quad \frac{B(t)}{B_0} = C_R^2 \quad \frac{p(t)}{p_0} = C_R^5 \quad \frac{\beta(t)}{\beta_0} = C_R$$

As β will increase linearly, initial parameters must be chosen carefully to avoid β-limit issues.

- **Non-ideal scaling with cooling and resistive flux loss**, $T \sim C_R^{\epsilon}, \epsilon \leq 2$

Magnetic flux decays according to $\frac{\partial\psi}{\partial t} = -\frac{\eta\lambda^2}{\mu_0}\psi$ with time constant $\tau_\psi = \frac{\mu_0}{\eta\lambda^2}$

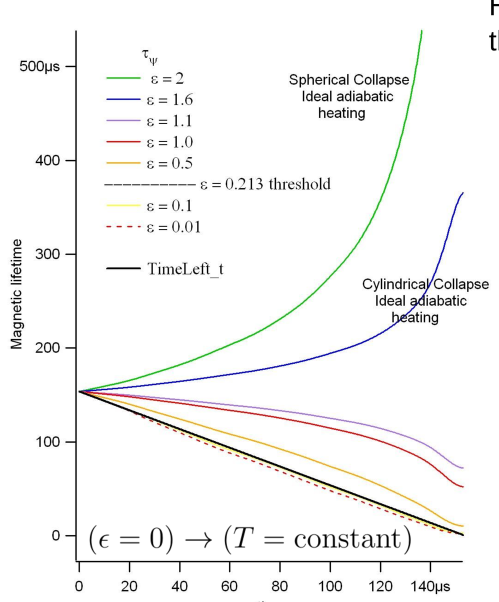

Here λ = 4.493/*R(t)* is the magnetic eigenvalue, and η is the resistivity which scales according to Spitzer formula:

$$\eta \sim T^{-3/2} \sim C_R^{-3\epsilon/2} \text{ and } \lambda \sim C_R$$

Then the magnetic lifetime scales as:

$$\tau_\psi \sim C_R^{(3\epsilon/2-2)}$$

One pessimistic case is an isothermal scenario ϵ = 0 then $\tau_\psi \sim C_R^{-2}$ and the field vanishes before the compression is complete. Only when ϵ > 0.213 will the field survive the compression. In the optimum spherical compression with adiabatic heating and no cooling, the magnetic lifetime will increase as:

$$\tau_\psi \sim C_R$$

These limiting cases are distinct enough that magnetic measurements during actual compression experiments should indicate the magnitude of cooling effects. However, in practice there exist confounding effects such as impurity level increase causing resistive loss due to the Z_{eff} dependence, as well as possible changes in the radial profile of plasma current that changes B_{wall} without changing the flux Ψ, and so it is important to have a complete diagnostic program that directly measures T(t) and n(t). Still, simple scaling models are very illuminating to compare to the full set of these measurements.

REFERENCES

APS DPP 2016, General Fusion Presentations

Monday, October 31, 2016, 2:00 PM–5:00 PM
1. P. O'Shea, et al. **CP10.00103** : Acoustically Driven Magnetized Target Fusion At General Fusion
2. R. Ivanov, et al. **CP10.00106:** Plasma Studies in the SPECTOR Experiment
3. W. Young, **CP10.00107 :** Thomson Scattering Results from General Fusion's SPECTOR
4. M. Reynolds, et al. **CP10.00108 :** Simulation of MTF experiments at General Fusion
5. C. Dunlea, et al. **CP10.00105 :** Magnetic Compression Experiment at General Fusion

Tuesday, November 1, 2016, 2:00 PM–5:00 PM
6. K. Ross ,et al. **JP10.00078** : Spheromak Plasma Cooling through Metallic Spallation

SUMMARY OF DESIGN ITERATIONS

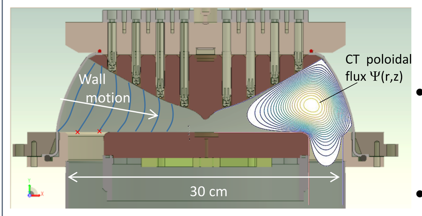

PCS 1 (5/2012, MRT 4738)

- 2 mm thick Al flyer plate, 30 deg, spherical section. Flyer plate edge runs tangent to wall to avoid jetting, but lower edge shears away from outer wall at first movement.
- Bare copper inner flux conserver with central gap
- 16 Surface magnetic probes, 2 interferometer chords, Neutron scintillators , bubble tubes.
- Spheromak eigenvalue λ = 58 m^{-1}, Ψ = 17 mWb of poloidal flux, n_e = 5x10^{21} m^{-3}
- Compression time of 44 μs, Total CT magnetic lifetime of 60 μs.

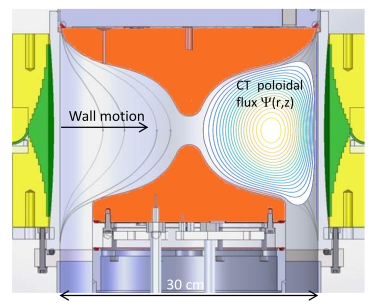

PCS 2, 3 (6/2013, 9/2013 MRT 10151, 14772)

- 3.5 mm and then 7 mm thick Al flyer plate using hyperboloid implosion geometry, no shearing.
- Bare copper inner electrode shape avoids contact with FP.
- Titanium gettering system with 3 retractable Ti-balls
- Added 3rd interferometer, Ion Doppler, multi-exposure survey spectrometer set, and total visible light emission vs time.
- Spheromak eigenvalue λ = 35 m^{-1}, Ψ = 16-18 mWb of poloidal flux, n_e = 2x10^{21} m^{-3}
- Compression time = 63 μs (PCS2), 83μs (PCS3), Total CT magnetic lifetime of ~200 μs.

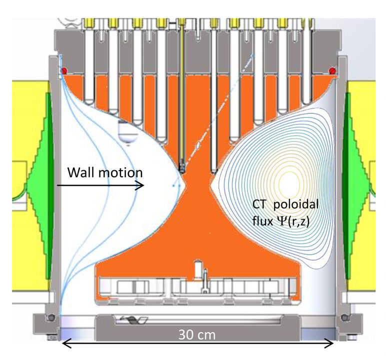

PCS 4, 5, 6, 7 (12/2013 – 8/'14) MRT: 4, 6; MRST: 5, 7

- 7mm thick Al flyer plate using hyperboloid geometry, inner surface was diamond turned (to remove microtexture) starting on PCS6 to try to minimize microdebris injection.
- Inner electrode has central shaft and voltage gap below spheromak region (aka Chalice design), to reduce tilt instability
- Explored wall materials (Cu and Al) & coatings (W, e-plated Cu)
- Gettering with Ti (PCS 4,5) and Lithium (PCS7), none on PCS6
- Added two B probes at r = 17 mm, X-ray photodiodes,

X-ray pinhole imaging with Phantom camera, and magnetic signal "Veto" safeguard on HE
- With PCS5, began running as "sustained spheromak", driven by ~2ms pulse of ~150 kA.
- Spheromak eigenvalue λ = 37 m^{-1}, Ψ = 16 – 25 mWb of poloidal flux n_e = 2x10^{20} to 2x10^{21} m^{-3}
- Compression time of 83 μs, Total CT magnetic lifetime of 300 μs – 500 μs. $T_e(0)$ ~ 100 eV

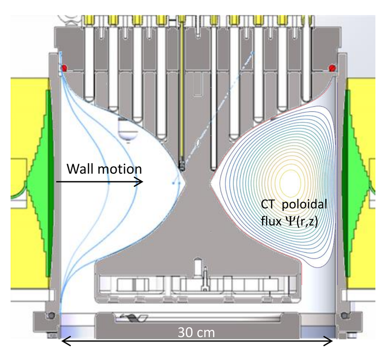

PCS 8, 9, 10 (12/2014 – 5/2015) MRT: 8 & 9; MRST: 10

- Inner electrode of Al with plasma-sprayed W coating.
- Gettering with Lithium, 3 retractable Li-sticks.
- Flyer plate driven by shockless acceleration on PCS 9 and later, this is to minimize ejection of microdebris.
- Ion Doppler begins to watch Li II line at 548 nm.
- Sustain current 120 kA for PCS 8, 9, and 125 kA for PCS 10
- Ψ = 8 – 16 mWb of poloidal flux, n_e = 2x10^{20} to 5x10^{20} m^{-3}
- Compression time of 83 μs, Total CT magnetic lifetime of 300 μs – 600 μs. $T_e(0)$ > 150 eV

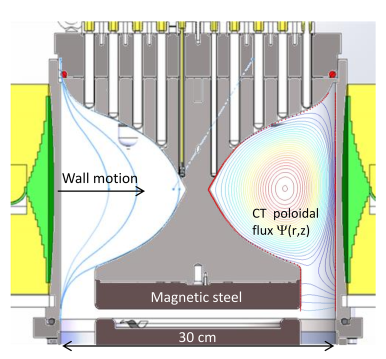

PCS 11 (7/2015, MRT 33525)

- Bottom plate of Inner electrode made of W-coated magnetic steel to focus a bridge of magnetic flux across gap. This was done to cause a natural MHD barrier for residual free-wheeling edge current, with the purpose of maintaining high edge q-values without applying external sustainment drive
- Changed B probe array to have a toroidal array of 6 probes at r = 52 mm, and also 3 probes on the bottom of the chalice.
- No Sustain current, Ψ = 19 mWb of poloidal flux, n_e = 2x10^{21} m^{-3}, $T_e(0)$ > 100 eV
- Compression time of 83 μs, Total CT magnetic lifetime of 600 μs.

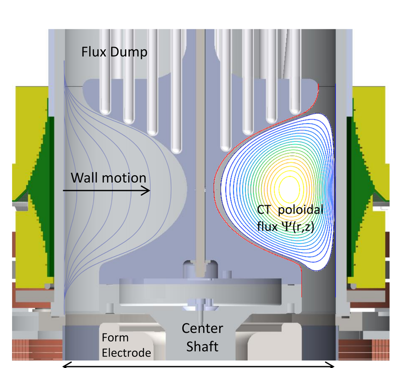

PCS 12 (11/2015, PROSPECTOR[1, 4] 10826)

- A major design change was made to explore spherical tokamak (ST) plasmas, formed by Marshall gun discharge into a pre-existing toroidal field created by external current driven on a separate center shaft electrode. This enables higher q and more stable plasma behavior, similar to CHI on other ST's.
- An upper volume was added to act as a "flux dump" so that vacuum toroidal field wouldn't block formation.
- I_{TF} = 492 kA, I_{plasma} = 200 kA, λ = 36 m^{-1}, Ψ = 15 mWb of poloidal flux, n_e = 1x10^{21} m^{-3}
- Compression time = 83 us, Total CT magnetic lifetime of 900 μs. $T_e(0)$ > 200 eV

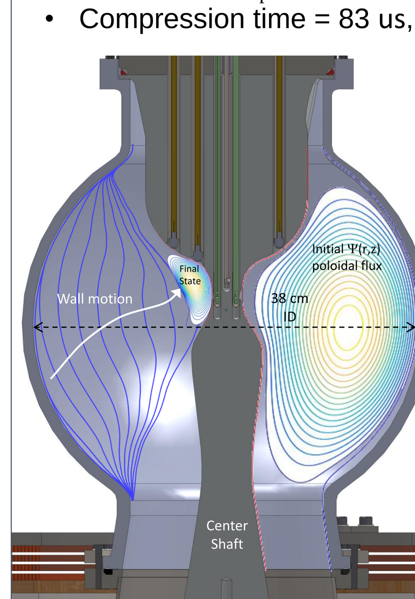

PCS 13 (9/2016, SPECTOR[2] 4915)

- Major change to a spherical flyer plate compression scheme, to keep plasma in a positive D shape for longer.
- SPECTOR also operates as a Marshall-gun initiated ST, like PROSPECTOR, having a center shaft for pre-formation toroidal field and a separate formation electrode. The gap between center shaft and formation electrode was 30 cm further down than previous to lessen possible impurity injection from electrode arcs.
- Diagnostics are similar to previous machines
- I_{TF} = 380 kA, I_{plasma} = 250 kA, n_e = 1x10^{20} m^{-3}, $T_e(0)$ > 300 eV
- λ = 26 m^{-1}, Ψ = 20 mWb of poloidal flux
- Compression time = 160 μs, Total magnetic lifetime = 1.3 ms
- Basic machine design will be used for future tests.

RESULTS

Improvement in poloidal magnetic lifetime and compression factor

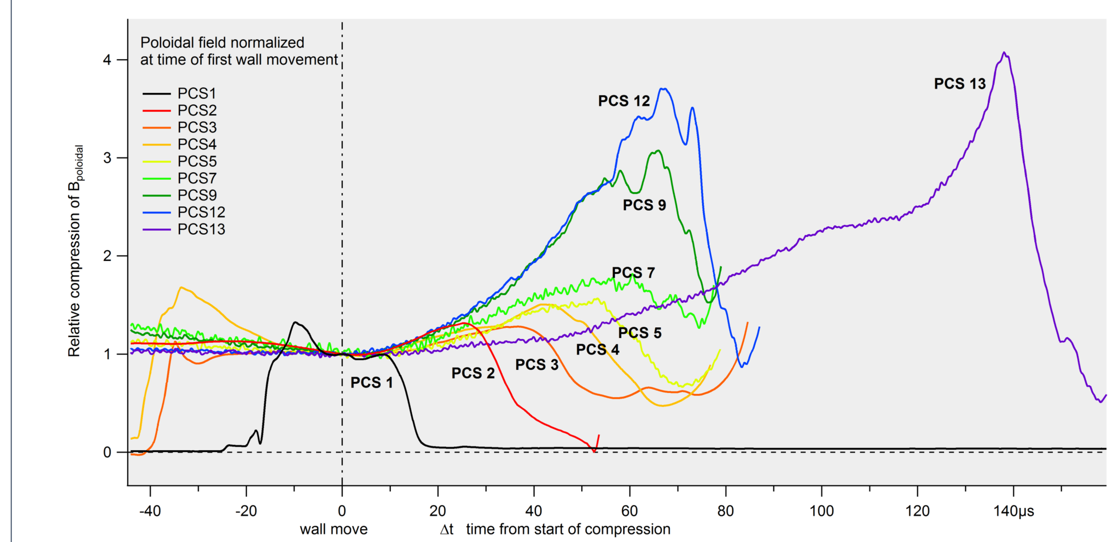

To see the progression of improvements during the PCS campaign, all of the poloidal magnetic data has been time-shifted to be aligned at the start of compression or "wall move". They are normalized at that point to show relative field increase. Each trace is the toroidal average of the set of B-probes at r = 26 mm, or the nearest equivalent position for that device. We find that sustained spheromaks (PCS9) and two variations of spherical tokamak configurations (PCS12 & PCS13) can have sufficiently good magnetic and thermal lifetimes that MTF compression physics can be explored. Wall conditioning and control of gas input play important roles in achieved results. At peak compression the max B_{pol} fields range from 1-2 Tesla within the PCS shots.

Peak magnetic compression ratio

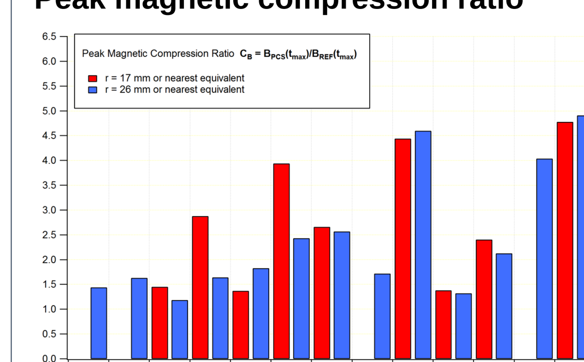

It is important to understand if the act of compressing the plasma causes a change in the poloidal flux decay rate. And so it is informative to examine the ratio of peak B_{pol} on a PCS shot to the value of B_{pol} at the same time (t_{max}) on an identical non-compressed reference shot.

$$C_B = \frac{B_{PCS}(t_{max})}{B_{ref}(t_{max})}$$

This ratio is graphed on the left for each of the PCS shots, for the inner radius poloidal B-probes. Wall motion results in a radial shift in the magnetic axis, as well as flux compression, and so probes at finite radius will have a maximum possible C_B value if flux is conserved and there is no profile change. Compression past that point reduces the field measured at that probe because $R_{axis} < r_{probe}$. For r = 26mm probes on PCS4-11 this ideal limit is C_B < 6, and C_B < 26 for r = 17mm. Thus PCS9 conserved (4.6/6) = 76% of its poloidal flux up to the first radial compression factor of R_0/R = 3, (r = 26mm), but then loses the rest in the next radial factor of 2. By the time the peak of wall field gets to r = 17 the flux is at roughly 15% of the ideal value. The flux conservation for the first radial factor of 3 of PCS9 is consistent with a compressional heating that scales as $T \sim C_R^{1.5}$, or a rise of core T_e from 100 eV to 520 eV.

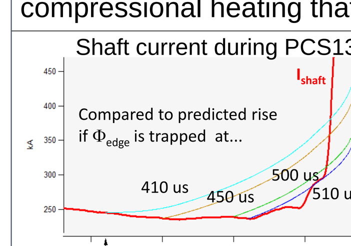

Toroidal flux loss into the gun During the compression, the coaxial inductance of the CT chamber is decreasing rapidly and edge toroidal flux Φ_{edge} is displaced into the gun section, while in the plasma Φ_{core} is better conserved, resulting in a growing poloidal current shell that becomes unstable[4]. Only at late time does the wall close off the gun and trap Φ_{edge}. Key effect on most PCS shots.

Comparison to equilibrium and MHD models

PCS 12 Magnetic data compared to models

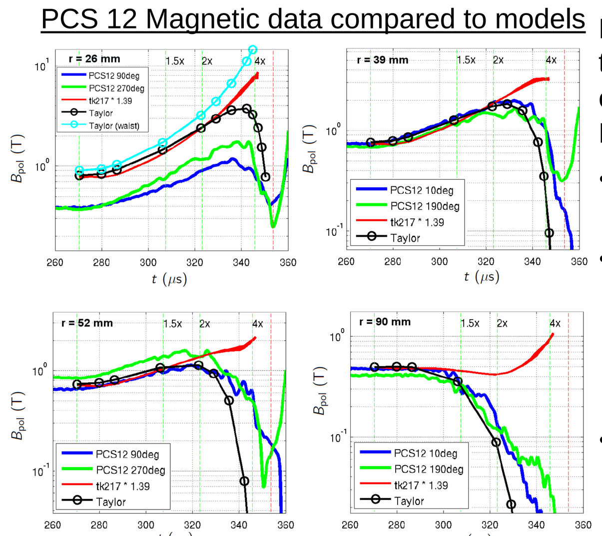

Here, B_{pol}(t) data at 4 radial positions is compared to both a Taylor state equilibrium model of constant Ψ = 15 mWb (black and teal), and a 3D MHD simulation (red) using VAC[4].
- MHD and Taylor models are scaled to match initial B_{pol} values at r = 39 mm position.
- Measured B_{pol} (blue and green) data matches model field strength profiles (t=270us) at all positions except r = 26mm, this could be due to a probe calibration error, or actually having a current profile outside of what was considered.
- The simple Taylor model is a better fit to PCS12 than the MHD simulation, and does not require flux loss to account for the drop in B, instead it is due to relative motion of peak B away from probe location, with the probe "walking" into a corner where B is small in any case. The high degree of flux conservation (r = 26mm has C_B = 4.03 which is 84% of the ideal limit of 4.75) is consistent with some heating, best matching a scaling of $T \sim C_R^{0.6}$, during the first radial factor of at least C_R = 3. This scaling was calculated using pre-compression τ_ψ = 876 μs. This would correspond to a core temperature rise from 200 eV to 386 eV due to compression, which is below the upper bound implied by non-detection of neutrons on PCS12.

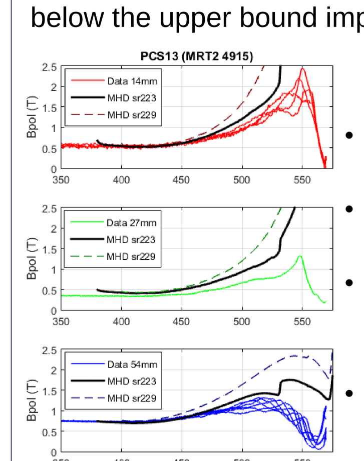

PCS 13 Magnetic data compared to MHD simulations[4]

B_{pol}(t) data from all 3 radial positions is compared to 2D VAC MHD.
- Magnetic field increase was higher in an initial attempt (sr229) at simulating this compression than was actually observed in PCS13.
- Initial attempt used a peaked current profile and has a large profile change during compression due to loss of edge toroidal flux.
- An improved match was found (sr223) when the initial current profile included a pre-existing shell of elevated plasma current due to on-going edge toroidal flux loss during the 400 μs after formation.
- Probe data develops a large 15% - 30% n=1 mode early on in the compression, which likely causes increased thermal transport from core to edge. 3D MHD simulations are required to predict instability.

Density rise, Interferometer data

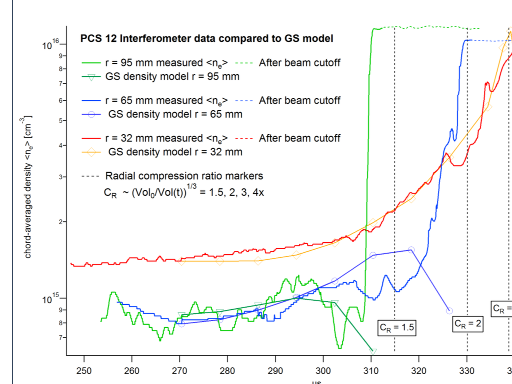

PCS12 chord-averaged electron density is measured by dual wavelength interferometers (1.55, 1.31 μm) at three radial locations r = {32, 65, 95} mm.
- Each chord is vertically oriented, double pass.
- Dual wavelength allows rejection of vibration.
- Density rise seen on PCS 12 was consistent with good conservation of core particle inventory
- Matches quadratic-profile Grad-Shafranov model (β_{axis} is rising from 4% to 17% in time, plus constant density of 10^{15} cm^{-3} on edge open field lines)
- Data shows small decrease below peak expected density, then a rise near wall before cutoff.

Ion Doppler data and conclusions about edge lithium transport

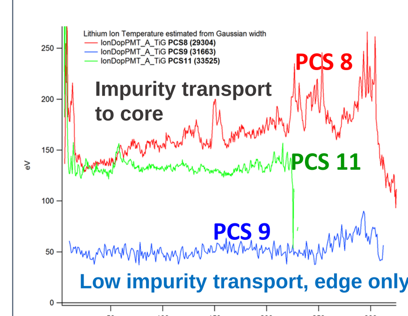

For PCS 8, 9, 11 and 13 the ion Doppler spectrometer was observing the line shape and brightness of the Li II line at 548 nm. This was to monitor possible flow of wall material into the core, as a possible source of cooling.
- In steady state conditions of the plasma core, lithium should fully ionize in < 10 μs, so its presence indicates a flow and recycling to and from the wall.
- The observed value of T_i gives an estimate of the maximum depth at which the Li ions transport is occurring.
- Line brightness also increases with ion transport depth, due both to light collection volume and increasing plasma density and T_e as fresh Li ions transport deeper into the core.
- Overall we saw PCS8 and 11 (and lab-shots leading up) have bright Li emissions with deep transport to the core (T_i > 150 eV), where as PCS 9 data was 5x dimmer and with Li ions only persisting near the edge (T_i < 50 eV). This may explain PCS9's superior performance during compression, due to better magnetic surfaces keeping heat in and impurities out.

Neutron diagnostics

Calibration setup with Am-Be source

Neutron bubble tubes

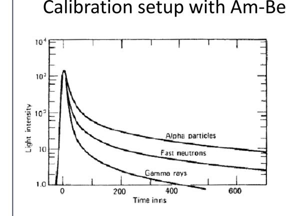

Pulse shape for BC501A liquid scintillator, in response to α, γ, and n particle impact.

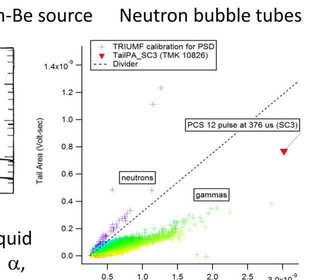

We monitor high energy (100 keV – 30 MeV) emission during the plasma shot with liquid (BC501A) and plastic scintillators using PMT detectors.
- Signals are digitized at 2 GHz during the shot so that digital pulse shape discrimination (PSD) can be used to distinguish between incident neutrons and photons, as well as measure their energy.
- Our detectors have been absolutely calibrated at the TRIUMF lab with an Am-Be source.
- Our most sensitive detector will observe 1 neutron detection for every 2000 emitted from the plasma, this threshold would equate to expected DD fusion yield at maximum plasma temperature of 500 eV for peak densities and dwell time during implosion.

CONCLUDING REMARKS

- On best shots plasma was stable during a compression factor of R_0/R >3.
- Magnetic field rise during compression is consistent with compressional heating that scales as $T \sim (R_0/R)^{1.33}$ or better while plasma is stable.
- Dominant thermal loss mechanisms seem to be a combination of large amplitude MHD instabilities that grow during compression, which enhance electron thermal transport, as well as the cooling effect of increased impurity transport from the edge to the core, which can arise both as an independent increase of ejection from the wall and also as a side effect of MHD activity. We are beginning to understand the mechanisms for these dominant effects and test out corrective actions.
- For the range of compression timescales we are considering, careful control of initial magnetic profiles and their evolution is key to demonstrating a window of parameter space where MTF can work.

FUTURE DIRECTIONS

- Compression within a metal flux conserver that remains connected to the formation Marshall gun generally does not compress toroidal flux as well as it compresses poloidal flux. This leads to a change in magnetic profile as current sheets form near the plasma edge, which can cause MHD instabilities that decrease confinement.
- Several strategies to better compress the toroidal flux and/or to compensate for edge flux loss during compression are being investigated. PCS 14 is planning to test one such approach.
- Significant work is currently being done to expand diagnostic capability on both lab-only and field-mobile experimental systems. The main objectives are to accurately measure the internal profile and magnetic structure of formation-only shots, as well as develop passive temperature diagnostics that can continuously monitor core plasma temperature during a compression experiment.
- As we learn more from these subscale PCS experiments, we hope to apply that understanding to plan a larger scale set of compression experiments [Plasma Compression Large, or PCL tests]. These will be closer to a full scale demonstration with significant fusion yield, which is expected to be possible with approximately 10 x increase in both magnetic flux, and plasma density, while keeping initial temperature and collapse time similar to PCS tests.
- Formation of this high density, high flux target plasma will be explored with the new Plasma Injector 3 (Pi-3) device currently beginning the construction phase.
- Results from the PCL MTF demonstration tests will be used to refine the design of a prototype MTF reactor with compression driven by converging acoustic pulses within liquid metal.